BULLFROG: ENABLING HIGH-RATE LOW-WASTE COMPOSITES MANUFACTURING

Innovate UK Project No: 10153656

University of Southampton

Project Deliverable for WP 2

February 2026

Industrial Partners:	Easol Limited, Brookhouse Aerospace
Academic Partners:	University of Southampton, Cranfield University,
Date:	09/02/2026

i. Contents

ii. Abbreviations & Nomenclature

NDT- Non-Destructive Testing
NDE- Non-Destructive Evaluation
AT- Active Thermography
PEEK- Polyetheretherketone
FRP- Fibre Reinforced Polymer
CFRP- Carbon Fibre Reinforced Polymer
BVID- Barely Visible Impact Damage
IR- Infrared
LVI- Low Velocity Impact
IRT- Infrared Thermography
PIRT- Passive Infrared Thermography
ERR- Energy Release Rate
DFPA- Detector Focal Plane Array
NIR- Near Infrared
SWIR- Shortwave Infrared
MWIR- Midwave Infrared
LWIR- Longwave Infrared
FIR- Far Infrared
InSb- Indium Antimonide
UAV- Unmanned Aerial Vehicle
VOx- Vanadium Oxide
NETD- Noise Equivalent Temperature Detectivities
FPN- Fixed Pattern Noise
OST- Optically Stimulated Thermography
PT- Pulsed Thermography
LPT- Long Pulsed Thermography
SHT- Step Heated Thermography
LIT- Lock-in Thermography
PPT- Pulsed Phase Thermography
FMT- Frequency Modulated Thermography
FFT- Fast Fourier Transform
DFT- Discrete Fourier Transform
SST- Spot Scanning Thermography
LST- Line Scanning Thermography
PSMR- Pseudo-Static Matrix Reconstruction
DPPT- Dynamic Pulsed Phase Thermography
ECST- Eddy Current Stimulated Thermography
VT- Vibro-Thermography

Executive Summary

Project Bullfrog aims to enable high-rate, low waste production of advanced composite structures by utilising Active Thermography (AT) to produce a low cost, Non-Destructive Testing (NDT) system. This will enable understanding of manufacturing defects via in-situ testing. The primary breakthrough is the use of lower cost uncooled (i.e. microbolometer) thermal imaging cameras and robust signal processing pipelines to remove the reliance on more expensive and operationally complicated cooled photon detector cameras to both qualitatively and quantitatively detect common manufacturing defects seen in composite materials.

A brief overview of composite materials and the most common manufacturing and in service damage types are presented, as well as how they impact residual strength of composite materials. This document delivers the state of the art in terms of pulsed thermographic experimental practises and why AT is positioned as the optimal NDT solution for high-rate composite material inspection compared to other NDT techniques. A comparison and validation of the industrial use case of using uncooled vs cooled camera systems is examined and commonly used signal processing methods in relation to Pulsed Thermography (PT) are documented.

The technical and economic feasibility of using uncooled microbolometers for industrial composite NDT is validated by numerous studies demonstrating that, when paired with robust signal processing, these systems deliver performance comparable to cooled counterparts. Future work for Project Bullfrog will focus on the optimisation of experimental excitation parameters (standoff distance, power delivery, and pulse length), which seem to vary considerably in the scientific literature depending on specimen material, geometry and defect types. Generalising these parameters remains the biggest challenge in producing a robust NDT system.

1. Introduction

Non-Destructive Testing & Evaluation (NDT & E) techniques are extremely valuable methods for analysing the structural health of engineering structures without cutting apart or altering the material. Therefore, their non-invasive nature allows for characterisation of the structure while it is still in service, minimising operational downtime and eliminating the costs associated with sampling structural components. Additionally, NDT & E serves as a robust predictive tool as it can effectively identify a wide range of structural defects, from manufacturing of the component until the end of its operational life. This approach provides a wealth of information about how design choices can influence the lifetime of the structure and fundamentally, how damage propagates in engineering structures [1].

The understanding of damage propagation becomes even more relevant in the area of composite materials, due to their inherent anisotropic structure. Composite materials are composed materials made up of two or more constituent materials, which combine to form a material that is superior to its individual components. Composite materials have seen wide success in aerospace, automotive and maritime industries in recent years due to their superior specific strength compared to more dense metallic materials [2]. This, however, comes at a cost, as the damage accumulation is non-trivial; hence the growing important partnership between composite materials and NDT & E techniques.

NDT & E technology has steadily matured over the last couple of decades and now encompasses a wide range of techniques all with differing qualitative and quantitative abilities. A non-exhaustive list of NDT & E techniques used today are visual inspection, ultrasonic testing, liquid penetrant testing, radiography and holography [3]. Among the NDT & E techniques, there is also Active Thermography (AT). AT is rapidly growing in science and engineering due to the promising properties it has over other NDT & E techniques. Specifically, its non-contact and non-invasive nature allows for highly efficient data acquisition and simplified experimental setups compared to methods requiring physical coupling or intrusive access. This can potentially allow for easier generalisation of the experimental set-up for a diverse range of materials and geometries, proving highly advantageous for the development of a robust NDT & E system.

2. NDT & E Techniques

Non-Destructive Testing (NDT) and Non-Destructive Evaluation (NDE) are essential two sides of the same coin. NDT refers to the act of discovering defects itself via the testing configuration and is the procedural side of the field. It involves specialised equipment like ultrasonic sensors, X-rays, thermal cameras etc. to inspect a material. NDT is concerned primarily with qualitative analysis and the identification of a flaw or discontinuity. NDE on the other hand is analytical in nature and it post processes the data taken from NDT to quantitatively examine the physical characteristic of the defect, including its size, location, orientation etc. These two terms are often used interchangeably, and the combined approach will be referred to as NDT from here on out.

NDT techniques can be broadly divided into contact techniques and non-contact techniques. Contact methods require adequate contact between the sample and the sensor to obtain reliable data. Non-contact methods do not require physical contact between the sensor and the sample, which massively widens the use space for non-contact NDT. The “big five” NDT techniques that dominate the market are eddy current, ultrasonic, magnetic testing, radiography and liquid penetrant testing [4]. Ultrasonic testing made up 36% of the market share in 2023, showcasing its dominance in the industry. Ultrasonic testing can detect mainly sub surface defects and is used extensively in the aerospace and oil/gas industries but is largely a manual process, which is highly dependent on the operator’s skill level. This limits the ability to automatically inspect large areas efficiently, which is often required in high throughput composite manufacturing like aerospace or wind industries [5]. Eddy current testing is capable of detecting flaws on surface coatings like paint, but it limited to the testing of electrically conductive materials. Magnetic testing is limited to detecting anomalies on or close to the surface of ferromagnetic materials and testing of complex shapes may not be possible. Radiographic inspection is also capable of detecting sub surface features but has safety considerations, can be expensive, time consuming and largely dependent on the orientation of anomalies. Lastly, liquid penetrant testing is used for surface inspection of mass-manufactured products and is a messy process which is largely stochastic as too many variables affect the test.

It can be seen that the various techniques are well established to fill certain niches. For example, liquid penetrant testing is low cost and essential for steel/welding processes, ultrasonics for its portability to be used in oil and gas piping and magnetic testing for surface defects in ferromagnetic materials. There exists a niche in composite manufacture and operation processes. Composite structures require a highly mobile and efficient NDT system. AT has the

advantage of being able to be completely automated if the signal processing is adequately understood, as well as being non-contact. Unlike ultrasonic testing, AT is not restricted to point source scanning and has a wider field of view. Additionally, the thermal properties of composite materials can help contrast the defect, enhancing detection. This makes AT a prime candidate for facilitating high throughput characterisation of large-scale composite structures.

3. Composite Materials and Defects

Composite materials on a fundamental level are composed of two phases, a reinforcing phase (the fibres) and a continuous phase (the matrix). Modern day composites combine many different constituents for either phase. The main types for the reinforcing phase are carbon, glass or aramid fibres. For the continuous phase the prevalent forms are thermosetting resins made from epoxy or thermoplastic resin systems like Polyetheretherketone (PEEK). The landscape of these material constituents is vast, and the classification of composite materials is shown in Figure 1 [6].

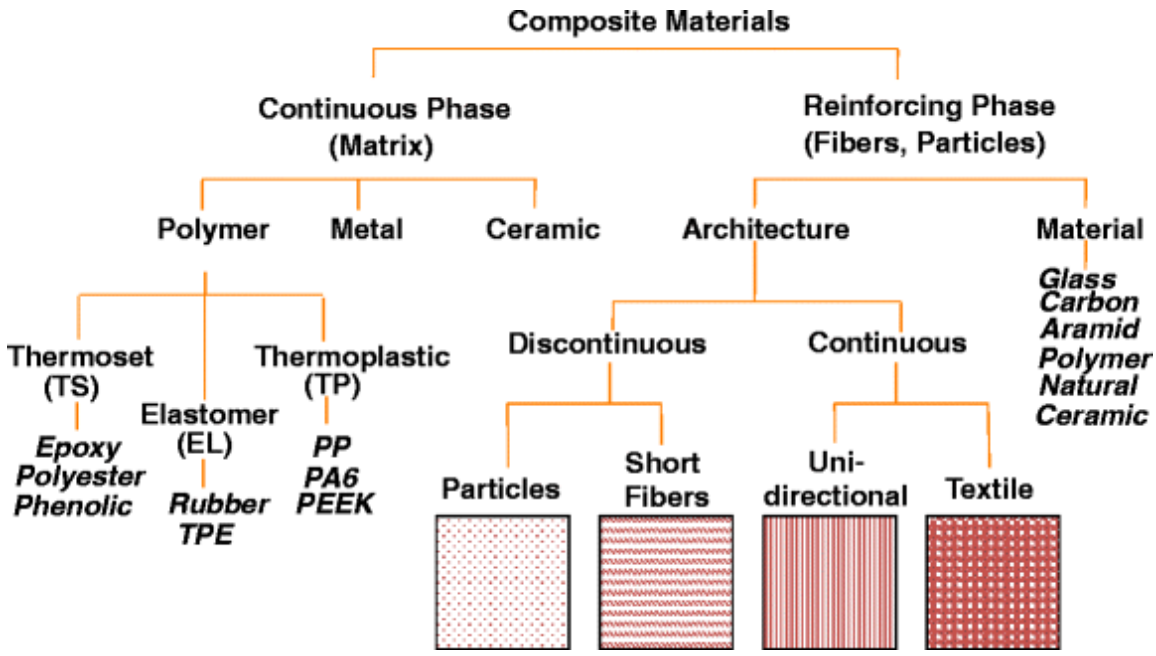

Figure 1. Classification of Composite Materials [6].

Composite material popularity has exploded in recent years and for good reason. Aerospace and automotive applications require materials which have high specific strength and stiffness. Fibre Reinforced Polymer (FRP) composite materials fill this need excellently, with a tailored Carbon Fibre Reinforced Polymer (CFRP) laminate offering 2-5 times the specific strength compared to a similar weight aluminium component. Aircraft manufacturers in particular are increasingly moving away from metallic components in favour of composite materials due to

the potential weight savings that can be gained from composite materials. Any weight reduction in the air, directly translates to less fuel consumption for airliners and more profitable aircraft. Figure 2 shows the material constituents of the Boeing 787, composites make up to 50% of the mass of the structure, this can save up to 20% in weight compared to traditional aluminium structures [7].

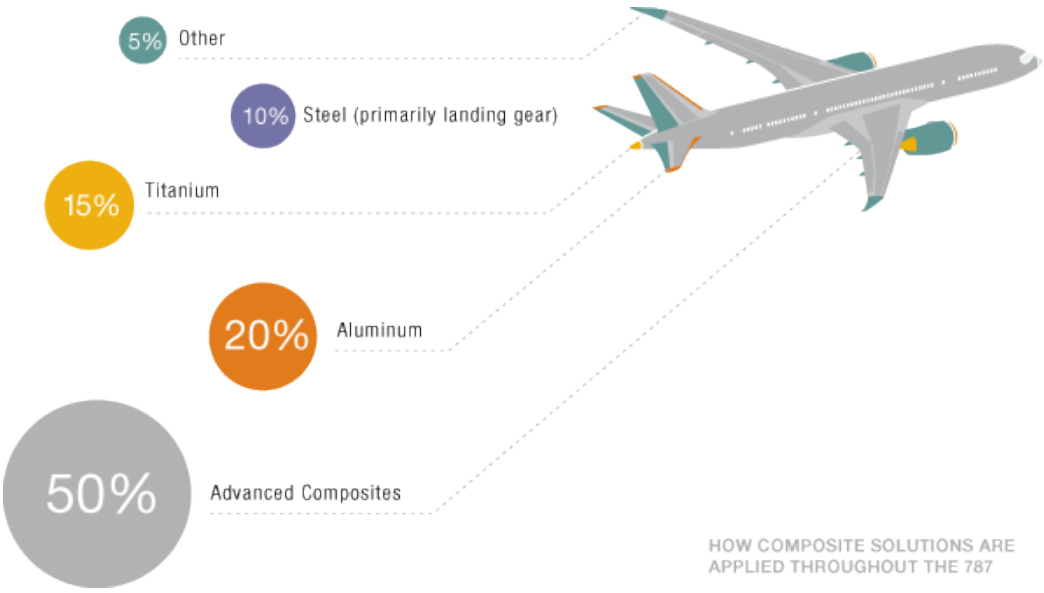

Figure 2. Material Make-up of Boeing 787 [7].

FRP composite materials have numerous variables in their material makeup. These variables include but are not limited to:

- Stacking sequence
- Ply thickness
- Ply architecture
- Material Constituents
- Processing techniques

The result of this is a material unlike homogeneous metallics where the deformation is well defined. Hence, understanding damage accumulation both in manufacture and in operation is a non-trivial task. Composite materials are anisotropic as their material properties differ depending on the direction of measurement. Composite structures can vary infinitely, and the composite designer varies the above parameters depending on the needs of the laminate. As such, understanding how defects form during manufacture and during service is of critical

importance to composite structure manufacturers, so that the manufacturing processes can be optimised and the lifetime of the structure extended.

The defects are numerous as well as the sources of those defects, owing to the structure of the material. Manufacturing defects are grouped into three main categories and a lot of the defects are shown in Figure 3:

- Matrix defects
- Fibre defects
- Interface defects.

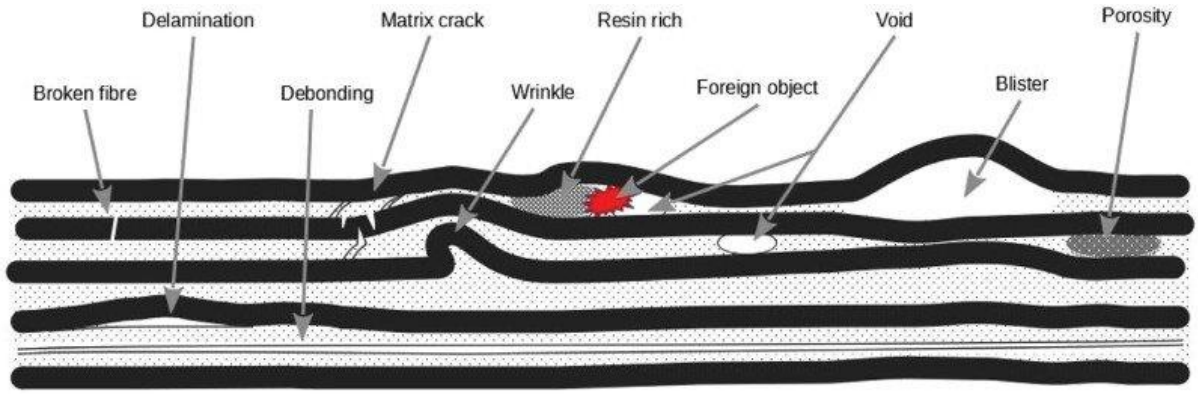

Figure 3. Common Manufacturing Defects Found in FRP Composite Materials.

Each defect type can have serious implications for the residual strength of the composite structure. Matrix defects primarily consist of voids and incomplete curing. Voids are a serious problem in composite manufacturing and are manufacturing process independent (for example autoclave or resin transfer moulding). Voids shape and content influence the matrix dominated properties the most with a reduction in shear modulus and transverse modulus. If voids are present at a cracked interface they enhance the possibility of unstable crack growth. Fibre defects include wrinkles in larger laminates, commonly seen in larger laminate thicknesses seen in the wind industry. Other fibre defects include fibre misalignment, fibre breakage and irregular distribution of fibres within the matrix, creating weak spots in the laminate. Fibre misalignment and wrinkles can seriously reduce the compressive stiffness and strength of the structure therefore reducing the buckling resistance. Lastly there is interface defects which include unbonded regions on fibre surfaces and delamination between the plies of the laminate [8]. Delamination in particular is one of the most worrying failure modes in composite materials as it can effectively split the structure into separate sub structures which severely

reduces the overall load capacity of the structure [9]. Having an efficient and robust NDT method to track manufacturing defects in-situ is extremely promising in composite manufacturing. This can allow manufacturers to understand how their manufacturing parameters (vacuum, resin viscosity, pressure, temperature etc.) influence defect formation. Manufacturers could then optimise these parameters in house to improve the overall quality of their components and in turn increase the life span.

NDT is often used to access the structural health of composite components during planned maintenance cycles after a certain amount of in-service time. Common service induced damage include [10]:

- Impact damage
- Cyclical loading causing fatigue damage
- Unexpected out of plane and in plane overloading causing fibre failure or matrix/fibre debonding
- Bearing failures from stress concentrator features such as open holes

Impact loading is particularly worrying as it can cause Barely Visible Impact Damage (BVID) under Low Velocity Impact (LVI). This damage type is nearly undetectable to the naked eye but under the surface it presents various damage mechanisms including delaminations, which as stated before can seriously compromise the structural integrity of composite components. If left undetected and therefore unrepaired this damage can propagate according to the laws of fracture mechanics, and when the crack reaches a certain threshold, the crack can propagate unstably causing sudden catastrophic failure of the component [11]. This damage type can propagate unstably either due to unexpected overloading (on a wing on a particularly windy day) or else due to cyclic loading causing fatigue damage. This significantly reduces the residual strength of the overall structure. BVID can of course be characterised using sub surface NDT techniques like ultrasound or indeed AT and quickly being able to characterise a structure using NDT could also allow for more frequent maintenance, increasing the chances of detecting damage before it becomes critical.

4. Infrared Thermography Imaging Systems

Infrared Thermography (IRT) is an umbrella term used to describe all NDT techniques that use an infrared camera to register the thermal response of a material. This non-invasive technique is rapidly gaining popularity due to the advancement in thermal imaging technology in terms of, sensibility, spatial resolution, speed, data processing abilities and cost [12]. IRT is fundamentally composed of passive and active approaches shown in Figure 4.

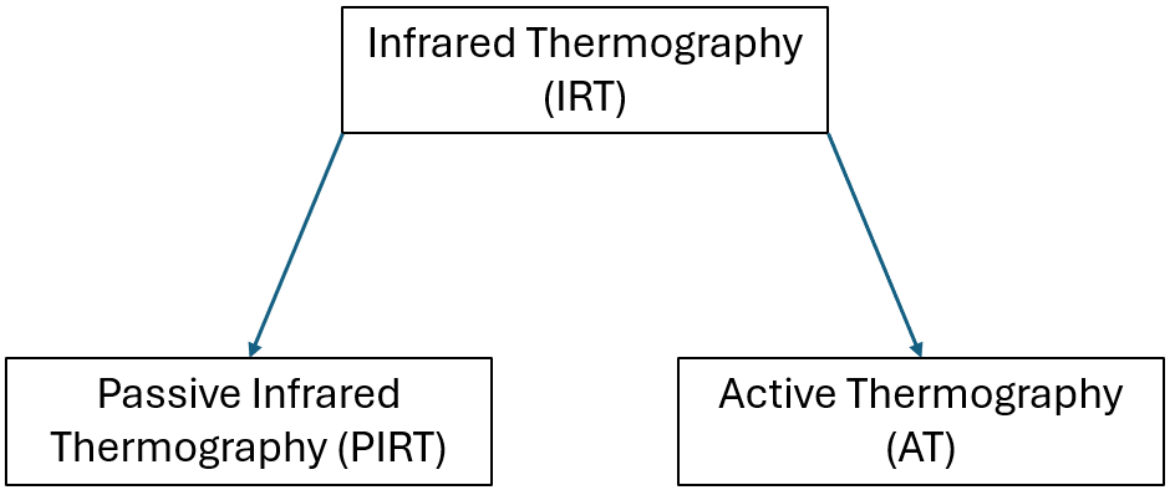

Figure 4. Family Tree of Infrared Thermography (IRT).

Passive Infrared Thermography (PIRT) uses infrared cameras to detect the non-equilibrium state of materials; these materials are usually not the same temperature as the surrounding environment they operate in. It can also be used to characterise the heat dissipation of a fracture process. According to the laws of fracture mechanics when a damage process happens, i.e. cracking or separation of an interface, some of the energy released is dissipated in the form of heat. This heat signature can contain a lot of information about the Energy Release Rate (ERR) of a material and be used in conjunction with computational modelling to accurately predict a materials response to propagating damage [13–15].

Active Thermography (AT) uses the same constituents only this approach induces a non-equilibrium state in the material via an excitation source. These excitation sources come in various forms and can use different laws of physics to induce this temperature change in the material. The temperature gradient on the medium surface is recorded and analysed by an IR (Infrared) camera to determine the structural integrity of the structure. As thermal waves flow

inside the material via diffusion, the temperature response will be different for an area containing a defect compared to the sound materials. This discrepancy is what allows for qualifying and quantifying material damage in structures. This mechanism allows for AT to have very competitive costs compared to NDT techniques like ultrasonics or radiographic systems [16,17].

IRT imaging systems are composed of three constituents, optical systems, detectors and the atmosphere. The optical system contains lens, prisms and mirrors with the intention to focus and concentrate the light (infrared radiation) from the sample onto the Detector Focal Plane Array (DFPA). The infrared detector is a sensor, which converts the intensity of the infrared radiation that is incident to the DFPA surface into a measurable electrical signal. The digitised signal is transformed to be intelligible on a screen. Detectors are designed to be sensitive to different ranges in the spectrum of infrared light. The electromagnetic spectrum for infrared light ranges from 0.7-1000 μm. The bands associated with the infrared spectrum are Near IR (NIR:0.7-1.4 μm), Shortwave IR (SWIR: 1.4-3 μm), Midwave IR (MWIR: 3-8 μm), Longwave IR (LWIR: 8-15 μm) and Far IR (FIR-15-1000 μm). For MWIR and LWIR the intensity of emissions and atmospheric transmittance is higher than others making these bands the most useful in IRT. Between 5-8 μm, no radiation is transmitted due to atmospheric absorption [18]. Figure 5 shows the electromagnetic spectrum with the infrared spectrum sub divided [19].

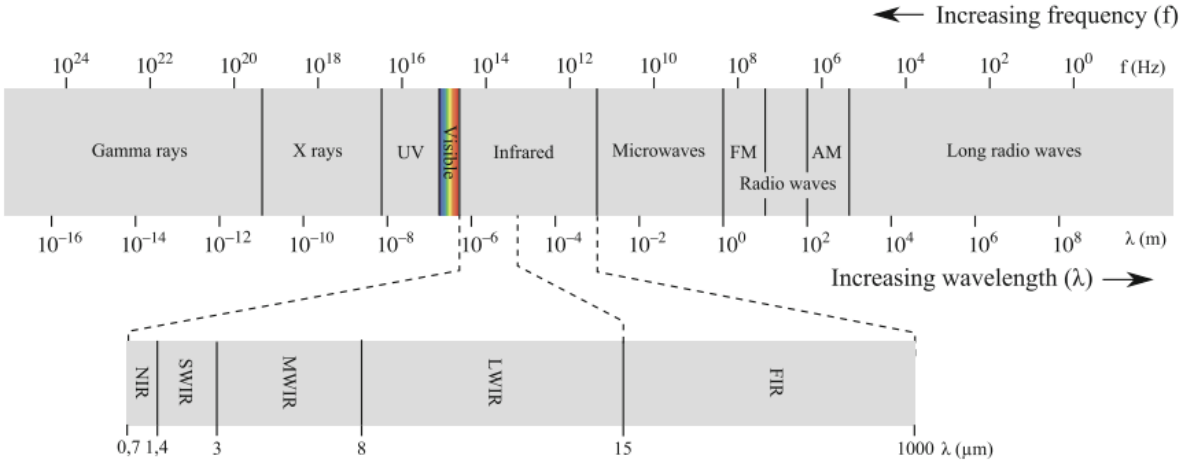

Figure 5. The Electromagnetic Spectrum with the Infrared Spectrum Sub Divided [19].

5. Cooled and Uncooled IR Cameras

There are essentially two types of optical detectors in IRT, photon detectors and thermal detectors. For photon detectors the radiation is absorbed within the material by the incoming photons interacting with electrons and knocking them into a higher energy state which creates an electric charge, this is known as the photoelectric effect. Photon detectors work primarily in the MWIR band between 3-5 μm due to atmospheric absorption. The most commonly used type of photon detector are Indium Antimonide (InSb) detectors. Photon detectors show good signal to noise ratio and are generally very sensitive to small fluctuations in temperature however to achieve this they must be cryogenically cooled using liquid nitrogen and cryocooler which increases complexity of the overall system and subsequently cost [18].

Conversely thermal detectors absorb incident thermal radiation directly, which changes the temperature of the detector material and subsequently its material properties and an electrical output is generated. Thermal effects are independent of spectral wavelength, however these types of detectors operate most effectively in the LWIR band. Cryogenic cooling is not required for these detectors, vastly expanding they're operational use case. Thermal detectors can be further sub divided into three groups:

- Thermopile- This is basically a collection of thermocouples. Thermocouples in series can achieve better temperature sensitivity.
- Pyroelectric detectors- Internal variance in the internal electrical polarisation is calculated.
- Bolometers- These tend to be the most widely used thermal detectors. Variance in the electrical resistance, voltage or current is transformed into electrical output which is processed into an image.

The introduction of uncooled thermal detector cameras brought IR imaging to the masses. Thermal detectors have benefitted hugely from advances in semiconductor manufacturing and micromachining which has allowed for smaller features to be produced on large arrays at lower costs, this revelation drives todays uncooled thermal detectors. Several studies have investigated the specific trade-off between uncooled thermal detectors and cooled photon detectors. Deane et al. [16] quantitively investigated the comparison between uncooled microbolometers and cooled InSb detectors to detect impact damage in aerospace grade composite materials. The study also investigated the influence of seven commonly used signal to noise ratio definitions. The findings concluded that the cooled camera offered higher raw

sensitivity which is expected. Conversely, the uncooled camera when paired with adequate signal processing, provides satisfactory results offering a lightweight alternative which could be implemented into a mobile thermal platform like an Unmanned Aerial Vehicle (UAV). Rajic et al. [20] compared between several commercially available vanadium-oxide (VOx) microbolometers (uncooled) and scientific grade InSb cooled systems. The systems were tested on a uniaxially loaded plate with a stress concentration feature which was a circular hole, this specimen was representative of an aircraft wing skin coupon. Rather unusually, the uncooled microbolometer consistently outperformed the cooled system for scan durations of 1500 load cycles or more. This is despite, the uncooled system having a Noise Equivalent Temperature Detectivities (NETD) that was 2-6 times inferior to the cooled system. Interestingly, the study dictates that NETD specifications have limited value as a sensitivity metric. This is because the noise for a cooled system is dependent on Fixed Pattern Noise (FPN). For an uncooled system the noise is inherently random and can be robustly reduced via advanced signal processing. As more data is collected with the uncooled system the noise declines and follows a log linear rate, eventually outperforming the cooled system. The contrast in the spectral response is considered between cooled MWIR and uncooled LWIR detectors [21]. There seems to be an “f-number” trade off. Uncooled sensors require fast lenses (low f-number) to compensate for lower sensitivity, while cooled sensors can get away with smaller cheaper optics at higher f-numbers for the same level of detection at long ranges [21]. However, this doesn’t take into consideration the impact of signal processing to remove the inherently random noise associated with uncooled sensors. The cost effectiveness crossover point was explored between cooled and uncooled camera systems for long range surveillance. Cooled cameras were seen to be cheaper for shorter ranges, whereas cooled systems were most cost effective at ranges exceeding 5km [22].

The literature seems to suggest that uncooled cameras are a cost-effective way to maintain high imaging quality especially in the face of advanced signal processing techniques. Still, to best optimise the usage of uncooled cameras, the lens system should have a sufficiently low “f-number”. The cost of an uncooled camera increases significantly with focal length, the same cannot be said for a cooled camera system as higher “f-number” can be accepted because the exposure time can be increased to keep the same radiation throughout. For very large focal lengths, cooled cameras will become cheaper than uncooled cameras and is only relevant for long range applications like surveillance [19].

6. Active Thermography

As mentioned before AT, is a subdivision of IRT and requires an excitation source to induce a non-equilibrium state in a material. AT has rapidly advanced in recent years and encompasses a vast range of techniques. AT can be broadly grouped depending on the physical principle of the technique and the type of thermal source used. Figure 6 shows the family tree of AT, which is continually growing as more approaches are discovered.

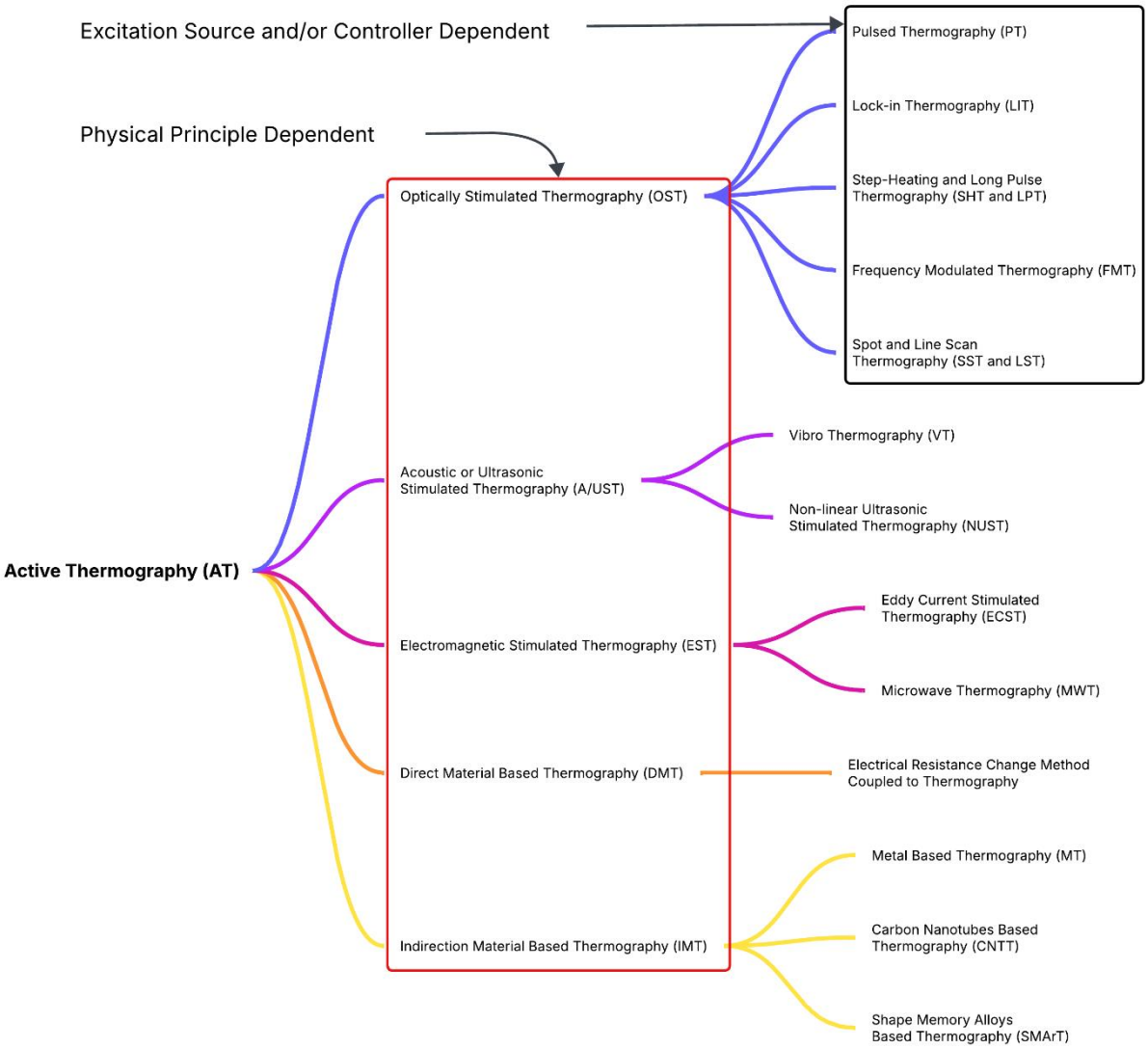

Figure 6. Family Tree of Active Thermography.

The most widely used and well-developed form is Optically Stimulated Thermography (OST), which uses an optical excitation source like halogen heat lamps (for periodic heating or longer pulses), flashes (for quick pulses) or lasers (fine control) to heat the surface of a material. Depending on the choice of excitation source and/or controller used the thermal signal that is

transmitted to the material can vary a lot and is shown graphically in Figure 7 as well as a standard experimental set-up for OST [17].

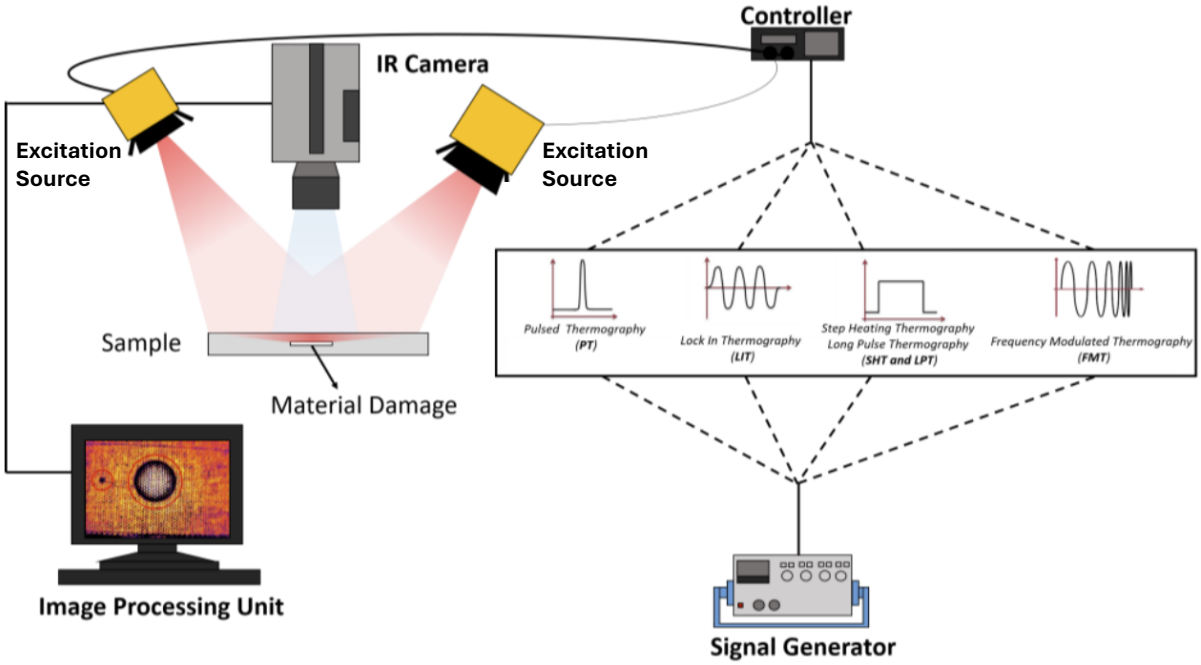

Figure 7. Standard Experimental Set-up for Optically Stimulated Thermography (OST) [17].

Pulsed Thermography (PT) and Long Pulse Thermography (LPT) both use a broadband signal from an excitation source like a Xenon flash tube or halogen lamp. In PT and LPT the duration and intensity of the pulse dictates the depth, resolution and material types that can be analysed. Xenon flash tubes provide significantly higher peak power over a shorter timeframe (~0.5 MW/m^2 in milliseconds) compared to halogen lamps (~30 kW/m^2 over several seconds to minutes). Xenon flash tubes are ideal for resolving shallow defects in thin or highly conductive materials like aerospace coatings. The shorter heating duration results in a concentration of higher frequencies which dissipate quickly in the material and do not have time to laterally diffuse. Conversely, Halogen lamps can penetrate deeper into the material due to the longer heating duration, which translates into a lower frequency dominated response. Lower frequencies have a larger thermal diffusion length, which results in them being able to travel further into the material without attenuating. However, the longer heating duration can cause lateral diffusion of heat which can reduce the contrast of defects compared to sound material [23]. Step Heating Thermography (SHT) slightly differs from LPT as the SHT data is measured during the application of the step pulse, whereas LPT data acquisition happens during the cooling phase. The aforementioned techniques operate in the temporal-temperature domain and

look at the pixel-by-pixel temperature history. Pulsed Phase Thermography (PPT) expands upon this via signal post processing of the incident thermal radiation, which enables phase analysis of the frequency domain. This solves the problem of heating inhomogeneity as the phase response is less sensitive to non-uniformity of heating, surface emissivity variations, and environmental reflections. Lower frequencies are used in PPT to assess deeper defects. To extract the phase from thermal data the Fourier Transform is used. The phase is essentially the time delay of the thermal wave as it propagated through a material and reflects off an internal boundary or defect etc. As the phase measures the timing of the thermal wave relative to the start of the excitation pulse it is intrinsic to the material. This allows for "slicing" through different depth in the material because different frequencies penetrate to different diffusion lengths. As the signal is broadband in pulsed thermography there can be a wide range of frequencies present, scanning through the phase response of these differing frequencies, allows for this "slicing" effect [17]. Hence PPT is a powerful post processing technique applied to pulsed thermographic practises. Table 1 provides a review of optically stimulated pulsed thermography (PT, LPT, SHT) experiments on composite materials in the literature including excitation source parameters, specimen details, camera parameters, defect types and outcome of study. The table shows how varied the experimental parameters are depending on specimen material and geometry and defect type. For instance, the standoff distance, which is the distance between the excitation sources and/or thermal camera and the specimen, to ensure a proper field of view and uniform thermal excitation, varies quite a bit. The non-exhaustive list of experimental procedures shown in the table indicate the standoff distance varies between 100 mm to 1000 mm, depending on the specimen properties and camera sensitivity etc. This is a critical parameter for optimisation because it influences the intensity of the thermal energy reaching the surface and the spatial resolution of the resulting data from the thermograms. Additionally, for LPT the power rating on the excitation sources (halogen lamps) varies between 500 W to 3400 W, not to mention the pulse duration in these instances. It is vital that a robust method is established to adequately determine the experimental parameters associated with the excitation source used.

Table 1. A review on Optically Stimulated Pulsed Thermography Experiments on Composite Materials in the Literature.

Author (Year)	Technique	Specimen (Material/Lay-up/Thickness/ Dimensions)	Excitation (Source/Power/Duration /Standoff)	Camera (Model/Type/Rate/Resolution)	Defect Types	Outcomes
Erazo-Aux et al. (2020) [24]	PT	CFRP & GFRP 10 layers 2 mm 300 × 300 mm Planar, curved, & trapezoidal geometries	2x FX60 BALCAR Flashes 12.4 kJ total (6.2kJ each) 2 ms 500 mm standoff	FLIR X6900 Cooled InSb 120/145 Hz, ~2000 frames 512×512	25 Teflon inserts per plate 3–15 mm lateral size 0.2–1.8 mm depth	Open-access dataset for algorithm testing. Provides raw data with non-uniform heating and noise. Facilitates characterisation of delaminations in complex geometries
Lopez et al. (2014) [25]	PT	CFRP 10-ply laminate 2 mm thick 300 × 300 mm	2x Balcar FX60 Flash lamps 12.8 kJ total (6.4 kJ each) 15 ms pulse Not specified	Santa Barbara FPA SBF125 Cooled Photon Not specified rate/frames 320×256	25 Teflon square inserts 3–15 mm lateral size 0.2–1.0 mm depth	Developing and validating a 3D finite volume method (FVM) model for composite inspection. The Behrens-theoretical conductivity model provided the most accurate agreement with experimental thermal decay.
Sirikham et al. (2019) [26]	PT	CFRP Unidirectional 8 mm thick 230 × 75 mm & 155 × 155 mm	2x Xenon Flashes (Thermoscope II) ~2 kJ total Short pulse (not specified) 250 mm standoff	FLIR SC7000 Cooled Photon 10 Hz, 900 frames 640×512	Flat-bottom holes 5–20 mm diameter 0.5–4.0 mm depth	Quantifying air-gap thickness from single-side inspection. Pearson correlation coefficients for thickness estimation reached 0.75 for blocks and 0.85 for holes. The thermal reflection coefficient (R) was found to vary linearly with depth but exponentially with thickness.

Moskovchenko et al. (2020) [27]	PT	GFRP (Glass Polyamide) Unidirectional prepreg 4-5 mm thick	Flash: 4x Xenon (24 kJ) 5–10 ms Laser: 300 W (935 nm) 0.4 s pulse 68×68 mm spot	ImageIR 6800/8800 Cooled scientific 5 Hz (Laser), 100 frames 1024×768 / 640×512	3 Delaminations from rear-notches Depths: 0.75, 1.2, 3.3 mm	Investigating GFRP semi-transparency effects on NDT. Laser heating yielded the highest SNR (84.6 vs 10.5 for flash at 0.75 mm). TSR derivatives significantly improved SNR for semi-transparent samples.
Kamińska et al. (2019) [28]	PT & SHT	Unidirectional GFRP 4.5 mm thick 205 × 205 mm	PT: 2x Xenon Flash (5 kJ). SHT: Halogen (2 kW) 10–16 s duration	PT: FLIR SC7000 (Cooled). SHT: IRS-320S-NDT (Uncooled) both 320×256	6 Flat-bottomed holes 4–16 mm diameter 1.0–3.5 mm depth	Comparison of PT and SHT. SHT achieved a higher detection rate (94%) than PT (88%), but PT sizing was three times more accurate. PT is ideal for near-surface flaws due to high initial SNR, while SHT is more reliable for deep defects as the thermal signal stabilises during longer heating.
Chrysafi et al. (2017) [29]	SHT & LPT	CFRP; 7 lay-ups (e.g. 0_2, $+-45_2$) 0.5–1.0 mm 220 × 100 mm	SHT: Heating element (ΔT=115 C) 2–2.5 min PPT: 750 W Lamp 2–3 s pulse 100 mm standoff	FLIR SC660 Uncooled ~15 Hz, 1500–2000 frames 640×480	17 Surface cracks (<0.1 mm deep) PTFE delaminations (3 x 4 cm)	Comparative analysis of 2D spatial vs 1D temporal processing. 1D techniques (Fourier/Wavelet) were 100% accurate for delaminations but failed for cracks. 2D spatial derivatives successfully revealed cracks by highlighting abrupt temperature changes at boundaries.

Pawar et al. (2016) [30]	PT & LPT	GFRP (10 mm) CFRP (4 mm) (210 × 280 mm)	GFRP: Halogen 30 kW in total (24 kW/m²) 5 s CFRP: Flash 3.2 kJ 5 ms 400 mm standoff.	NEC Avio TH-9100 Uncooled (Microbolometer) 10 Hz, 100–344 frames 320×256	Square holes (5–20 mm diameter) 2–6 mm deep Dis-bonds and 59 J impact damage	Normalising experimental sequences with synthetic 3D heat conduction models. Signal to noise ratio for defects improved from 16.8 to 24.6. Qualitatively, the method subdued non-uniform heating artefacts and resolved impact delaminations up to 2.27 mm deep that were invisible in raw data.
Wei et al. (2021) [31]	LPT	CFRP $[0_2/90_2/45_2/-45_2]$ 4 mm 250 x 80 mm	2x Halogen Lamps 2000 W (1000 W each) 10 s 1000 mm standoff	FLIR A6700SC Cooled InSb 20 Hz, 1000 frames 640x512	10 Flat-bottomed holes 5–25 mm diameter 1.5–3.0 mm depth	Improved depth accuracy from 20% error to 7% by correcting for 3D diffusion using a rectification method
Lizaranzu et al. (2015) [32]	PT, LPT	CFRP ($[0_{40}]$, 24 mm) Adhesive joint (GFRP, 5–20 mm) Sandwich (PVC core, 14 mm)	2x Halogen lamps 5000 W (2500W each) 3–110 s Not specified	FLIR P660 Uncooled Not specified, 450–750 frames 640×480	Realistic delaminations, inclusions (metal/latex), wrinkles, dry fibre, and adhesive voids	Evaluating NDT capabilities on wind turbine materials. Successfully detected defects at 2–3 mm depth in CFRP. Transmission mode proved superior to reflection for thick (10 mm) adhesive joints. Sandwich structures yielded clear dry-fibre defects.

Wang et al. (2018) [33]	PT, LPT & SHT	CFRP (7.3 mm) and GFRP (3 mm) Lay-up not specified 150 × 100 mm	PT: 6 kJ Flash LPT/SHT: 2x 1 kW Halogen 5 ms (PT) or 7 s (LPT/SHT) ~300 mm standoff	CEDIP Jade Cooled (Photon) 50 Hz, 1500 (PT/LPT) or 350 (SHT) frames 320×240	Flat-bottomed holes 2.5–10 mm diameter 0.5–2.5 mm depth	Quantitative comparison of LPT, PT, and SHT. Quantitatively, LPT with PCA identified 11/12 GFRP and all 8 CFRP defects, outperforming other methods. Qualitatively, LPT proved more effective for low-conductivity composites as halogen lamps provide ~4.6 times higher energy density than 6 kJ flashes.
Marani et al. (2023) [34]	LPT	GFRP 16.20 mm nominal thickness 315 × 170 mm	2x Halogen lamps 1000 W (500 W each) 225 s Distance set to limit max temp to ~42 °C	Flir A655sc Uncooled (Microbolometer) 1 Hz, ~1900 frames 640×480	Circular flat-bottom holes 7.86–17.40 mm diam. 0.50–11.85 mm depth	Automatic depth classification using blind linear unmixing and support vector machine. Achieved 96.18% balanced accuracy. High sensitivity (87.66%) for deep defects
Feuillet et al. (2012) [35]	LPT	Carbon/epoxy composite [0/+45/-45/90]S 2.35 mm thick 210 × 297 mm	2x Halogen lamps 1000 W (500 W each) 0.25–10 s Not specified	FLIR A325 Uncooled (Microbolometer) 4/40 Hz, 220 frames (at 4 Hz) 320×240	PTFE and P(E-TFE) polymeric disks 1 cm diameter 0.1 mm thickness	Low-cost halogen lamps and uncooled cameras. Identified defect depths with less than 12% error. Qualitatively, SVD analysis localised defects without prior knowledge, and front-face data alone proved sufficient for accurate parameter inversion.

Panella et al. (2021) [36]	LPT	CFRP; Various lay-ups (e.g. $[0/+45/-45/90]_{2/3}$) 3.0–7.7 mm 914.4 x 762 mm	4x Halogen lamps 4000 W (1000 W each) 5–6.25 s Not specified	FLIR A655sc Uncooled microbolometer 3–20 Hz, 150–625 frames 640×480	Polymeric inserts 5–25 mm diameter Delaminations Large impact cuts Widespread porosity	Evaluating industrial defect detection using established (TSR, PCT) vs proposed Local Boundary Contrast (LBC) techniques. LBC enhanced SNR for small 5 mm flaws, while statistical methods best mapped diffused porosity
Grosso et al. (2016) [37]	LPT	GFRP concentric adhesively bonded tubular joint pipe (5 mm thickness) & collar (12 mm thick) 101.6 mm pipe diameter 1 mm epoxy layer	2x Halogen lamps 6800 W (3400 W each) 30 s duration Reflection mode Standoff not specified	Uncooled microbolometer FPA 30 Hz, ~1800 frames 640×480	1 mm thick “lack of adhesive” transverse and longitudinal orientations	Validating 3D FEA models for thick industrial tubular joints. The defect detection limit was established in the range of 6–12 mm. Qualitatively, defects were clearly detectable at 6 mm depth (inner inspection) but were masked by the 12 mm collar thickness in outer inspection.
Wang et al. (2022) [38]	LPT	CFRP 11 mm thick 230 × 230 mm	2x Quartz Halogen lamps 2000W (1000 W each) **~2 kW/m²** 6 s pulse 45° dual-lamp setup	CEDIP Jade MWIR 5 Hz, 300 frames 320×240 300 mm standoff	24 Flat-bottomed holes 10, 14, 20 mm diameter 1.0–5.0 mm depth	Proposing three analytical models for depth retrieval. The 2D axisymmetric model reduced depth prediction errors to within 9%. The contrast time slope was confirmed to be proportional to depth squared but independent of defect size.

Lock-In Thermography (LIT) and Frequency Modulated Thermography (FMT) can both use the same hardware as the previously mentioned pulse techniques, only the signal is modified by a controller. In LIT the intensity of the signal is modulated periodically at a specific fixed frequency. All other frequencies that are not at the set frequency are cancelled out and what is left is the amplitude and phase of the thermal response at that set specific frequency. This allows for a narrowband signal, which can deliver more thermal energy to a specific depth in the material and has extreme sensitivity. However, it is slower than PT and if the user doesn't know what depths the defects are potentially located at, it can be time consuming to perform many heating cycles at different frequencies. If PT is used first for a broadband search of potential defects and followed up by LIT this could potentially allow for more quantitative analysis of the defect. The negatives of using a fixed excitation frequency seen in LIT is directly challenged in FMT. FMT uses a sweep of frequencies in a specific band (0.01 Hz to 0.1 Hz over 100 seconds for example) to excite the sample. The temporal-temperature data is processed using a Fast Fourier Transform (FFT) to extract the necessary phase information at the desired constituent frequencies. This allows FMT to resolve defects at various depths in the material in one excitation cycle. FMT, still requires a controlled stimulus over a relatively long duration and can be computationally challenging [39]. PT is still the fastest and most computationally efficient method to screen for unknown defects.

One of the shortcomings with the aforementioned techniques like PT, SHT, LIT and FMT is that the excitation sources produce a uniform area of heating across the surfaces of the material. This is ideal for detecting defects which lie in a plane parallel to the surface like delamination (interlaminar) or dis-bonding of interfaces between an adhesive and composite. Intralaminar damage or damage that is in a plane that is perpendicular to the surface is not detectable with traditional methods of OST. Figure 8 shows the ply level failure modes of FRP composite materials. Intralaminar cracks can be detected if the heating is localised. Although these damage types are energetically unfavourable compared to interlaminar damage (lower fracture toughness), they can still be present to various degrees especially in impact loading conditions.

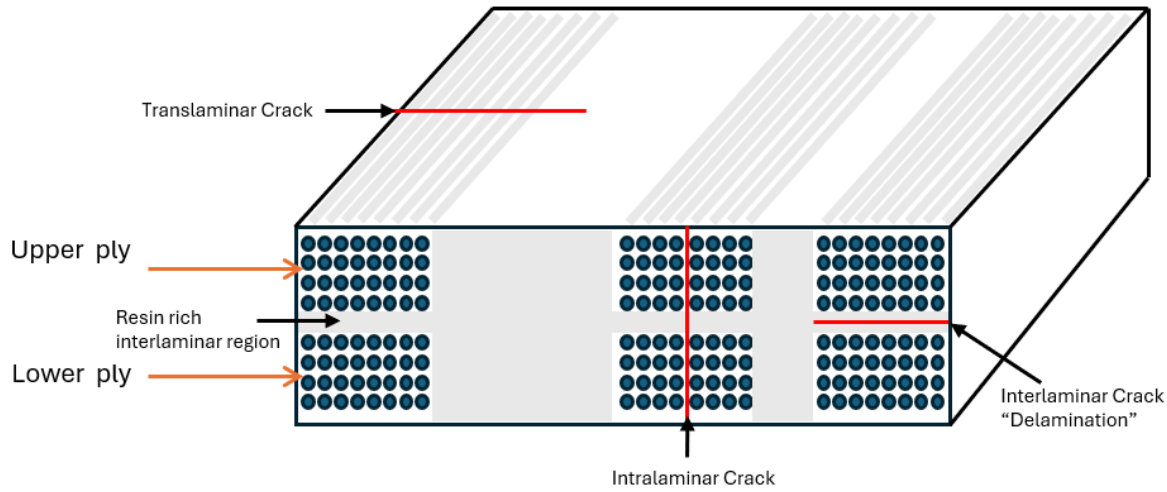

Figure 8. Ply Level Failure Modes seen in FRP composite materials.

Spot Scanning and Line Scanning Thermography (SST and LST) have been developed for this reason and damage is detected by an increase of apparent temperature or a change in the shape of the application heat. A complete inspection is achieved by processing images together in a chain as the heat source or the specimen are moved relative to each other at a constant rate. This motion (scan velocity) enables a relatively high rate of coverage compared to other excitation methods and positions SST and LST to be fully automated. From this point of view the heating response is dynamic and requires spatial temporal reconstruction to construct the individual frames into a single high-resolution map of the component. This process is not trivial and is the greatest challenge associated with SST and LST [40]. Traditional reconstruction methods use Pseudo-Static Matrix Reconstruction (PSMR) to stitch moving frames together into a single static data stream. PSMR is notoriously computationally expensive and requires precise controls over scan velocity and thermal camera frame rates. It also has to be done when the complete scan is finished and cannot be processed in situ. This does not allow for real time feedback and increases the data burden. Moran et al. [40] investigated the use of Dynamic Pulsed Phase Thermography (DPPT); this technique uses the time shift property of the Discrete Fourier Transform (DFT) to process the data, which allows it to be done on a buffer of frames that facilitates in-situ processing and damage detection. Interestingly, static features like heating line or random camera noise do not follow the cyclic periodic phase pattern in the scanning direction. Therefore, they postulate the dynamic nature of the process can be used to filter out randomly distributed noise.

The various methods above show the vast landscape in the optically stimulated domain and each of these techniques can be applied to other physical principles too. For instance, the literature documents use cases of pulsed, frequency modulated and lock in principles applied to Eddy Current Stimulated Thermography (ECST), as well as Vibro-Thermography (VT) to name a few. AT depends on the physical principle, excitation source and the control of the signal used. AT is becoming an increasingly robust NDT method and as the signal processing is becoming more established, the industrial use case for this technology is becoming more relevant with each passing year.

7. Signal Processing Techniques

Data obtained from the AT process is often contaminated with a plethora of different noise sources including, variations in the optical properties of the material, external reflections and non-uniform heating depending on the excitation method. These noise effects can complicate the defect detection and analysis process and making the AT process robust to a wide range of experimental parameters is an active area of research [41]. Signal processing of the thermal response of the material has been widely developed to reduce noise in thermal imaging, which has made each AT approach more adept in dealing with noise. A comprehensive review of data processing techniques was conducted in [23]. The commonly applied techniques used in PT are presented below in Table 3.

Table 3. Commonly applied signal processing techniques in Pulsed Thermography.

Signal Processing Method	Description
Thermographic Signal Reconstruction (**TSR**)	Fits a low-order polynomial function to the temperature cooling profiles. TSR can significantly reduce noise in thermal images and produces time-derivative images without generating additional noise. The time-derivative images can reduce the prevalence of the noise generated from non-uniform heating and background reflection. They provide good sensitivity to smaller and deeper defects. This technique does not make use of spatial information, only temporal.

Differential Absolute Contrast (**DAC**)	Very well-known technique. It uses the difference between the temperature of a sound area of material compared to a defected area.
Principle Component Thermography (**PCT**)	It uses Singular Value Decomposition (SVD) to reduce a matrix of thermal observations into orthogonal functions called principal components. It provides an excellent representation of both spatial and temporal features. It can significantly improve thermal contrast for subsurface defects and can help quantitatively estimate average flaw depth. This method is computationally expensive and does not provide an indication of actual damage distribution
3D Normalisation Algorithm (**3DNA**)	Supresses surface clutter caused by uneven heating and lateral heat diffusion. It is a reference free method and does not require a sound material reference point. It compensates for background non-uniformity in glass and carbon fibre composites. It is however highly dependent on accurate thermal material properties which are not always easy to obtain in anisotropic materials. It is also computationally expensive.
Multi-dimensional Ensemble Empirical Mode Decomposition (**MEEMD**)	Used alongside TSR to effectively differentiate the low-frequency background and high frequency noise from the informative aspect of the signal. This improves the damage detection capabilities in PT.

Gapped Smoothing Algorithm (**GSA**)	It is a 2D, reference free quantitative method to identify sub surface defects. It calculates a damage index pattern based of the real and estimated temperature profiles for every pixel. It can enhance the thermal contrast between sound and defected material and can suppress the effect of non-uniform heating. It can improve the damage detection far from the heating surface,
Partial Least Squares Thermography (**PLST**)	It is a statistical processing technique which is based on the partial least squares regression that computes new thermal sequences by fitting surface temperature data with observation time. It filters unnecessary data while isolating significant signal variations by decomposing and recomposing data. It can significantly increase signal to noise ratio and preserves temporal information.
Coefficient Clustering Analysis (**CCA**)	Groups pixels with similar thermal characteristics into clusters based on their regression properties. It segments data by identifying regions with common cooling properties, effectively differentiating between sound and defective areas. It simplifies interpretation of large datasets by characterising damage into distinct zones. The accuracy of the clustering is dependent on the number of clusters and the regression model used. It can be computationally expensive when dealing with high resolution, long duration thermal data series.

The data processing pipeline used varies quite a bit and is always a balance between enabling robust defect detection and minimising computational expense. Signal processing has been extensively shown to improve the defect detection and signal to noise ratio of thermographic practices, especially in the face of non-uniform heating, emissivity variations, environmental reflections and surface geometry.

8. Conclusions and Perspective

This report presents the state of the art in the NDT & E of composite materials through the use of AT. In particular, the most encountered manufacturing and in service composite material defects were explored, and the use of uncooled thermal detector cameras and cooled photon detector cameras were documented. Additionally, a comprehensive evaluation into pulsed thermographic experimental practices was conducted, which included comparison between different PT techniques, differing excitation sources and camera parameters for various specimen geometries and defect types. A list of commonly applied signal processing methods used in PT was also examined.

Project Bullfrog's main breakthrough is that an uncooled microbolometer IR camara can be adequately applied to quantitively and qualitatively determine different defects that may present itself in the composite material manufacturing pipeline. This is to be achieved by the advanced signal processing pipeline that will be applied to Bullfrog's approach. This in turn will allow for high throughput and low waste manufacturing of composite aerostructures.

From the literature, it can be seen that the use of uncooled microbolometers is technically and economically suited for this task. While cooled photon detectors offer superior raw sensitivity, several studies have demonstrated that uncooled microbolometer systems, when paired with appropriate signal processing, deliver excellent results:

- Marani et al. [34] achieved a 96.18% balanced accuracy for deep defect classification in GFRP using an uncooled microbolometer.
- Feuillet et al. [35] demonstrated that low-cost uncooled cameras could identify defect depths with less than 12% error, proving that front-face data alone is sufficient for accurate inversion.
- Pawar et al. [30] utilised an uncooled microbolometer to resolve impact delaminations up to 2.27 mm deep that were invisible in raw data, improving the signal to noise ratio from 16.8 to 24.6 through 3D normalization.
- Panella et al. [36] successfully evaluated industrial CFRP components using uncooled sensors, showing that Local Boundary Contrast (LBC) techniques could enhance the detection of 5 mm flaws.
- Grosso et al. [37] established a defect detection limit of 6–12 mm for thick industrial tubular joints using an uncooled microbolometer FPA, validating its use for complex industrial geometries.

- Kamińska et al. [28] found that using an uncooled camera with SHT achieved a higher detection rate (94%) than flash-based PT, noting its reliability for deep defects where the thermal signal has time to stabilise.

These findings confirm that the Bullfrog approach, namely combining low-cost uncooled hardware with a robust processing pipeline, is not only viable but offers a significant strategic advantage for high-rate composites manufacturing. By leveraging uncooled technology, the project can deliver a mobile NDT system while reducing the financial and operational burden associated with cooled IR systems.

The inherent challenge going forward is how to generalise or have a systematic approach for detecting the most common defects in composite materials. Future work for Project Bullfrog will investigate the optimisation of source parameters (standoff distance, power delivery, pulse length etc.) with the objective to minimise the cost associated with the excitation source. For instance, cheaper, low power 500 W halogen lamps have been shown to be effective for quantitative defect characterisation in both thin and thick composite structures when coupled with uncooled microbolometers. In thin 2.35 mm carbon/epoxy laminates, such sources enabled the identification of defect depths with less than 12% error [35]. Furthermore, even in significantly thicker 16.20 mm GFRP composites, the application of 500 W halogens for extended durations (225 s) allowed for automatic depth classification [34].

This suggests that low-cost, low-power sustained excitation can provide sufficient energy density for deep penetration, provided the pulse characteristics is aligned with the specimen's thickness. Longer pulses however, could allow for lateral diffusion, reducing thermal contrast so these parameters are far from being understood from the point of view of generalisation. By exploring the relationship between power delivery and thermal transients, the optimal pulse parameters can be determined. This, combined with a parametric computational approach, could fully explore such relationship from the point of view of thermal energy delivery. An optimisation for a wide range of defects, geometries and materials, is critical to minimising the effects of higher noise floors of uncooled sensors, ensuring that high-rate NDT remains reliable, even when inspecting the full spectrum of possibilities in manufacturing of complex composite structures.

References

[1] Duchene P, Chaki S, Ayadi A, Krawczak P. A review of non-destructive techniques used for mechanical damage assessment in polymer composites. J Mater Sci 2018;53:7915–38. https://doi.org/10.1007/s10853-018-2045-6.

[2] Bhong M, Khan TKH, Devade K, Vijay Krishna B, Sura S, Eftikhaar HK, et al. Review of composite materials and applications. Mater Today Proc 2023. https://doi.org/10.1016/j.matpr.2023.10.026.

[3] Gupta M, Khan MA, Butola R, Singari RM. Advances in applications of Non-Destructive Testing (NDT): A review. Advances in Materials and Processing Technologies 2022;8:2286–307. https://doi.org/10.1080/2374068X.2021.1909332.

[4] Cawley P. Non-destructive testing-current capabilities and future directions. Proceedings of the Institution of Mechanical Engineers, Part L: Journal of Materials: Design and Applications 2001;215:213–23. https://doi.org/10.1177/146442070121500403.

[5] Jodhani J, Handa A, Gautam A, Ashwni, Rana R. Ultrasonic non-destructive evaluation of composites: A review. Mater. Today Proc., vol. 78, Elsevier Ltd; 2023, p. 627–32. https://doi.org/10.1016/j.matpr.2022.12.055.

[6] Friedrich K, Almajid AA. Manufacturing aspects of advanced polymer composites for automotive applications. Applied Composite Materials 2013;20:107–28. https://doi.org/10.1007/s10443-012-9258-7.

[7] Ramakrishnan PN. Composite Materials, Metals, And Ceramics Used in the Boeing 787-Materials Overview. Journal of Research in Science and Engineering 2024;6:57–62. https://doi.org/10.53469/jrse.2024.06(08).13.

[8] Talreja R. Manufacturing defects in composites and their effects on performance. Polymer Composites in the Aerospace Industry, Elsevier; 2019, p. 83–97. https://doi.org/10.1016/B978-0-08-102679-3.00004-6.

[9] Harizi W, Chaki S, Bourse G, Ourak M. Mechanical damage assessment of Glass Fiber-Reinforced Polymer composites using passive infrared thermography. Compos B Eng 2014;59:74–9. https://doi.org/10.1016/j.compositesb.2013.11.021.

[10] Frossard G. Fracture of thin-ply composites: effects of ply thickness. École Polytechnique Fédérale de Lausanne (EPFL)., 2017. https://doi.org/DOI:10.5075/epfl-thesis-8032.

[11] Shabani P, Li L, Laliberte J, Qi G. Compression after impact (CAI) failure mechanisms and damage evolution in large composite laminates: High-fidelity simulation and experimental study. Compos Struct 2024;339. https://doi.org/10.1016/j.compstruct.2024.118143.

[12] Alfredo Osornio-Rios R, Antonino-Daviu JA, De Jesus Romero-Troncoso R. Recent industrial applications of infrared thermography: A review. IEEE Trans Industr Inform 2019;15:615–25. https://doi.org/10.1109/TII.2018.2884738.

[13] Lisle T, Bouvet C, Pastor ML, Margueres P, Prieto Corral R. Damage analysis and fracture toughness evaluation in a thin woven composite laminate under static tension using infrared thermography. Compos Part A Appl Sci Manuf 2013;53:75–87. https://doi.org/10.1016/j.compositesa.2013.06.004.

[14] Hattiangadi A, Siegmund T. A thermomechanical cohesive zone model for bridged delamination cracks. J Mech Phys Solids 2004;52:533–66. https://doi.org/10.1016/S0022-5096(03)00122-4.

[15] Akgun S, Senol CO, Kilic G, Tabrizi IE, Yildiz M. A novel damage evaluation of CFRPs under mode-I loading by using multi-instrument structural health monitoring methods. Eng Fract Mech 2023;286. https://doi.org/10.1016/j.engfracmech.2023.109291.

[16] Deane S, Avdelidis NP, Ibarra-Castanedo C, Zhang H, Yazdani Nezhad H, Williamson AA, et al. Application of NDT thermographic imaging of aerospace structures. Infrared Phys Technol 2019;97:456–66. https://doi.org/10.1016/j.infrared.2019.02.002.

[17] Ciampa F, Mahmoodi P, Pinto F, Meo M. Recent advances in active infrared thermography for non-destructive testing of aerospace components. Sensors (Switzerland) 2018;18. https://doi.org/10.3390/s18020609.

[18] Alfredo Osornio-Rios R, Antonino-Daviu JA, De Jesus Romero-Troncoso R. Recent industrial applications of infrared thermography: A review. IEEE Trans Industr Inform 2019;15:615–25. https://doi.org/10.1109/TII.2018.2884738.

[19] Gade R, Moeslund TB. Thermal cameras and applications: A survey. Mach Vis Appl 2014;25:245–62. https://doi.org/10.1007/s00138-013-0570-5.

[20] Rajic N, Street N. A performance comparison between cooled and uncooled infrared detectors for thermoelastic stress analysis. Quant. Infrared Thermogr. J., vol. 11, Taylor and Francis Ltd.; 2014, p. 207–21. https://doi.org/10.1080/17686733.2014.962835.

[21] Gross Herbert, Blechinger Frits, Achtner Bertram. Handbook of optical systems. Volume 4, Survey of optical systems. Wiley-VCH; 2008.

[22] Richards A. Cooled versus uncooled cameras for long range surveillance. FLIR Commercial Vision Systems 2010.

[23] Vavilov VP, Burleigh DD. Review of pulsed thermal NDT: Physical principles, theory and data processing. NDT and E International 2015;73:28–52. https://doi.org/10.1016/j.ndteint.2015.03.003.

[24] Erazo-Aux J, Loaiza-Correa H, Restrepo-Giron AD, Ibarra-Castanedo C, Maldague X. Thermal imaging dataset from composite material academic samples inspected by pulsed thermography. Data Brief 2020;32. https://doi.org/10.1016/j.dib.2020.106313.

[25] Lopez F, De Paulo Nicolau V, Ibarra-Castanedo C, Maldague X. Thermal-numerical model and computational simulation of pulsed thermography inspection of carbon fiber-reinforced composites. International Journal of Thermal Sciences 2014;86:325–40. https://doi.org/10.1016/j.ijthermalsci.2014.07.015.

[26] Sirikham A, Zhao Y, Nezhad HY, Du W, Roy R. Estimation of Damage Thickness in Fiber-Reinforced Composites using Pulsed Thermography. IEEE Trans Industr Inform 2019;15:445–53. https://doi.org/10.1109/TII.2018.2878758.

[27] Moskovchenko AI, Vavilov VP, Bernegger R, Maierhofer C, Chulkov AO. Detecting Delaminations in Semitransparent Glass Fiber Composite by Using Pulsed Infrared Thermography. J Nondestr Eval 2020;39. https://doi.org/10.1007/s10921-020-00717-x.

[28] Kamińska P, Ziemkiewcz J, Synaszko P, Dragan K. Comparison of Pulse Thermography (PT) and Step Heating (SH) Thermography in Non-Destructive Testing of Unidirectional GFRP Composites. Fatigue of Aircraft Structures 2019;2019:87–102. https://doi.org/10.2478/fas-2019-0009.

[29] Chrysafi AP, Athanasopoulos N, Siakavellas NJ. Damage detection on composite materials with active thermography and digital image processing. International Journal of Thermal Sciences 2017;116:242–53. https://doi.org/10.1016/j.ijthermalsci.2017.02.017.

[30] Pawar SS, Vavilov VP. Applying the heat conduction-based 3D normalization and thermal tomography to pulsed infrared thermography for defect characterization in composite materials. Int J Heat Mass Transf 2016;94:56–65. https://doi.org/10.1016/j.ijheatmasstransfer.2015.11.018.

[31] Wei Y, Zhang S, Luo Y, Ding L, Zhang D. Accurate depth determination of defects in composite materials using pulsed thermography. Compos Struct 2021;267. https://doi.org/10.1016/j.compstruct.2021.113846.

[32] Lizaranzu M, Lario A, Chiminelli A, Amenabar I. Non-destructive testing of composite materials by means of active thermography-based tools. Infrared Phys Technol 2015;71:113–20. https://doi.org/10.1016/j.infrared.2015.02.006.

[33] Wang Z, Tian GY, Meo M, Ciampa F. Image processing based quantitative damage evaluation in composites with long pulse thermography. NDT and E International 2018;99:93–104. https://doi.org/10.1016/j.ndteint.2018.07.004.

[34] Marani R, Campos-Delgado DU. Depth classification of defects in composite materials by long-pulsed thermography and blind linear unmixing. Compos B Eng 2023;248. https://doi.org/10.1016/j.compositesb.2022.110359.

[35] Feuillet V, Ibos L, Fois M, Dumoulin J, Candau Y. Defect detection and characterization in composite materials using square pulse thermography coupled with singular value decomposition analysis and thermal quadrupole modeling. NDT and E International 2012;51:58–67. https://doi.org/10.1016/j.ndteint.2012.06.003.

[36] Panella FW, Pirinu A. Application of Pulsed Thermography and Post-processing Techniques for CFRP Industrial Components. J Nondestr Eval 2021;40. https://doi.org/10.1007/s10921-021-00776-8.

[37] Grosso M, Lopez JEC, Silva VMA, Soares SD, Rebello JMA, Pereira GR. Pulsed thermography inspection of adhesive composite joints: computational simulation model and experimental validation. Compos B Eng 2016;106:1–9. https://doi.org/10.1016/j.compositesb.2016.09.011.

[38] Wang Z, Wan L, Zhu J, Ciampa F. Evaluation of defect depth in CFRP composites by long pulse thermography. NDT and E International 2022;129. https://doi.org/10.1016/j.ndteint.2022.102658.

[39] Ghali VS, Mulaveesala R, Takei M. Frequency-modulated thermal wave imaging for non-destructive testing of carbon fiber-reinforced plastic materials. Meas Sci Technol 2011;22. https://doi.org/10.1088/0957-0233/22/10/104018.

[40] Moran J, Rajic N. Remote line scan thermography for the rapid inspection of composite impact damage. Compos Struct 2019;208:442–53. https://doi.org/10.1016/j.compstruct.2018.10.038.

[41] Yang R, He Y. Optically and non-optically excited thermography for composites: A review. Infrared Phys Technol 2016;75:26–50. https://doi.org/10.1016/j.infrared.2015.12.026.